Observationally constrained reconstruction of 19th to mid-20th century sea-ice extent off eastern Greenland

Danielle A.M. Hallé, Nanna B. Karlsson, Anne Munck Solgaard and Camilla S. Andresen

Arctic sea ice has a significant impact on the global radiation budget, oceanic and atmospheric circulation and the stability of the Greenland ice sheet (Vaughan *et al.* 2013). Prior to the era of aircraft and satellite, information on sea-ice extent relied on observations from ships and people living at the coast. This information is a valuable contribution to better understand the history of sea ice. However, the information exists in a range of formats, e.g., sea-ice extent before the late 1800s is typically reported in the literature as an annual index from a single geographical point or as hand-drawn maps. This makes it difficult to assess and compare data across time and space. The combination of digitised historical maps and single-point data makes the information more accessible and provides a record that can help understand the dynamics and processes of the climate and its interactions with the cryosphere (Chapman & Walsh 1993).

In this study, maps of sea-ice extent by Koch (1945) were digitised. We use these maps in combination with sea-ice charts from the Danish Meteorological Institute (DMI) and Koch's sea-ice index from 1820 to 1939, to map estimated sea-ice extent between Iceland and Greenland going back to 1821. This information has not been included in even the most recent databases of Arctic sea ice (Walsh *et al.* 2015, 2017). Furthermore, we extract time series of sea-ice extent at a number of locations and investigate the relationship between them.

Our observation area is along eastern Greenland, between the southern tip of Greenland at 59°46′N northwards to 77°21′N.

Digitising Lauge Koch's maps

Koch's (1945) monograph comprises over 400 small maps that show monthly sea-ice extent from 1877 to 1939. We digitised the maps for the months in those years that contained sea ice. The data used by Koch were compiled by Thoroddsen (1884) from annals that describe the sea-ice extent off Iceland. The final result is 134 digital maps showing sea-ice extent from 1877 to 1939. These maps are available for download at *http://dx.doi.org.pangaea.de/10.1594/PANGAEA.887453*

Reconstructing the extent of sea ice between Greenland and Iceland from Koch's index

Koch's monograph contains a sea-ice index that categorises the width of the ice belt off Iceland, based on observations from 1820 to 1939. The Koch index has three main categories from A to C and subcategories from 1 to 3 for each letter (Table 1). A represents a narrow ice belt year, B is a broad ice belt year and C depicts a very broad ice belt year. The number next to the letter indicates how far the sea ice spread off Iceland. A subcategory value of 1 means the ice did not reach Iceland, 2 means it had spread along the northern coast and 3 indicates it had spread down as far as the southern coast of Iceland. Koch described an A year as the least severe sea-ice

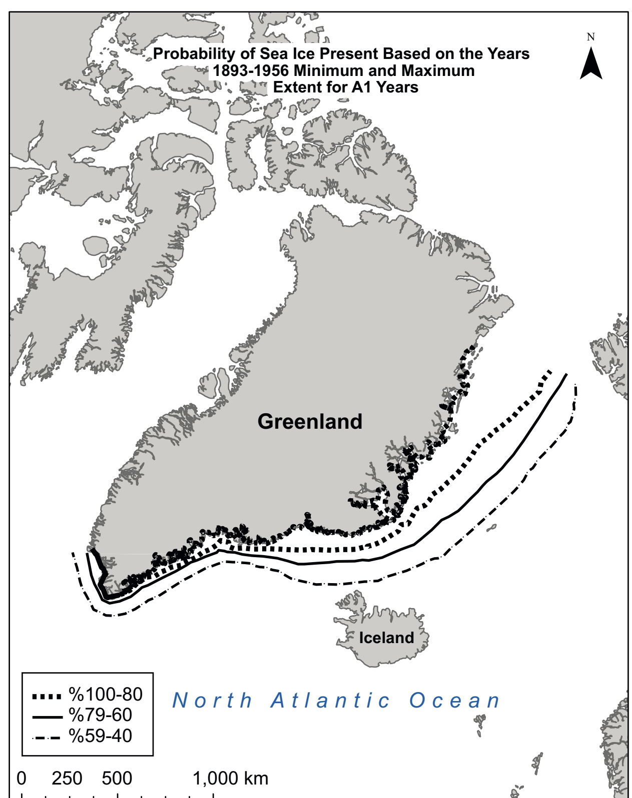

Fig. 1. Example of the final map, available for downloading, showing the probability of sea-ice extent based on historical maps from 1893 to 1956.

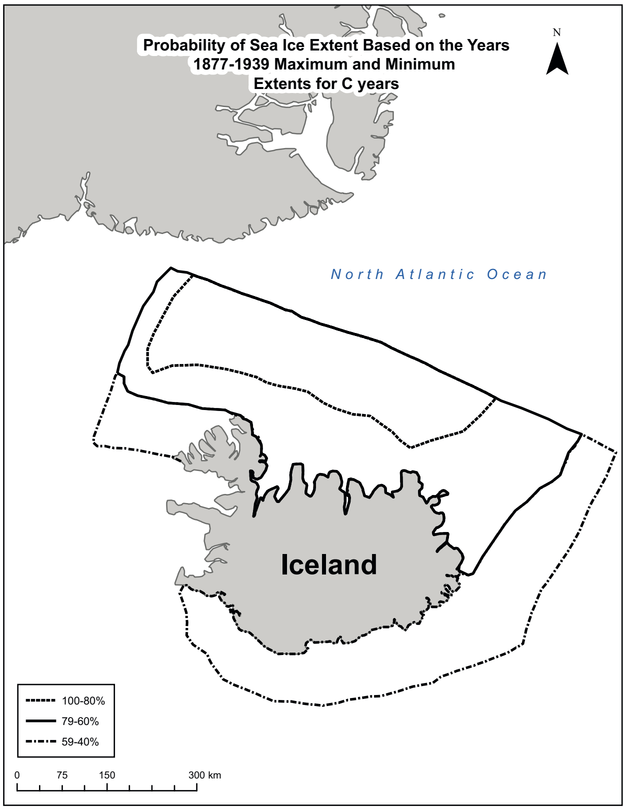

Fig. 2. Example of probability map of sea ice off Iceland 1877 to 1939.

year, whereas C is the most severe sea-ice year, with B being of intermediate severity. For example, the year 1895 is classified as B3 because it had a wider area of sea ice that touched on northern Iceland. Table 1 gives a summary of the index for each year. The duration of sea ice is not taken into consideration in these indexes.

The dataset we produced comes from three different sources of historical maps. The first is the digitised Icelandic maps, the second source is the DMI sea-ice charts that we digitised for 1893 to 1900 for the months between March and September each year. We have only digitised sea-ice extent along the east coast to the southern tip of Greenland from the DMI charts. These charts were based on ice conditions from variable sources such as land-based observations, scientific explorations and ship logs.

The third source is shapefiles from DMI that are available online. These files contain digitised sea-ice data from 1901 to 1956 (Underhill *et al.* 2014). We subsequently used these data to create the digitised maps. The DMI shapefiles were downloaded from the NSIDC at: *https://nsidc.org/data/G10007/versions/1*. The original maps used to create the shapefiles from 1893 to 1956 can be found on the NSIDC website: *https://nsidc.org/data/G02203/versions/1#*. Due to World War II, there is a gap in the data from 1939 to 1946.

Digitisation of the maps was done using ArcMap and exported as completed map files in jpeg format. Next, and for ease of data manipulation, the images were processed to convert the values into binary arrays, so that sea ice has a value of 1 and no sea ice has a value of 0. This was done in order to better visualise and plot the data. For each category (A1, A2…C) of the index, where there are at least 10 years present (Table 1) we created a map showing the probability that sea ice had a certain extent. The maps contain three lines of sea ice that depict 80–100%, 60–79% and 40–59% probability of sea-ice extent (Fig. 1). The percentages are calculations of the average sea-ice extent. We used the average sea-ice extent for each year belonging to each category to calculate the frequency of the extent. For example, the dataset shows that in 80–100% of those years within a certain category the sea ice extended to the thick dashed line, 60–79% of the time the extent reached the solid black line and only 40–59% of the time did the sea ice extend to the thin dashed line. The result of this procedure is six maps (A1, A2, A3, B1, B2 and C) from 1893 to 1956. In some cases, we can go even further back in time; three maps showing Iceland only (B2, B3 and C) have been constructed for the years 1877 to 1939. Figure 2 shows an example of a C year. There are no probability maps for A years for the Iceland-only maps, because of a lack of data.

Table 1. Summary of how Koch's index was classified for each year from 1821 to 1939

Index	A1	A2	A2	A2	A3	A3	B1	B1	B2	B2	B3	B3	B3	C	C	C
Year	1884	1823	1853	1924	1830	1902	1862	1913	1836	1916	1821	1861	1914	1822	1868	1911
	1922	1832	1867	1928	1831	1903	1876		1838	1917	1824	1870	1915	1828	1869	1918
	1926	1839	1899	1930	1835	1923	1877		1850	1921	1825	1875	1919	1837	1878	
	1927	1841	1904	1933	1854	1925	1879		1880	1932	1827	1883	1938	1840	1881	
	1931	1843	1905	1937	1864	1929	1889		1885		1829	1886		1855	1882	
	1934	1844	1908		1871		1889		1890		1834	1895		1856	1887	
	1935	1845	1909		1872		1893		1897		1857	1896		1858	1888	
	1936	1846	1910		1873		1894		1898		1859	1906		1865	1891	
	1939	1848	1920		1901		1900		1912		1860	1907		1866	1892	
Total	9			23		14		10		13			22			20

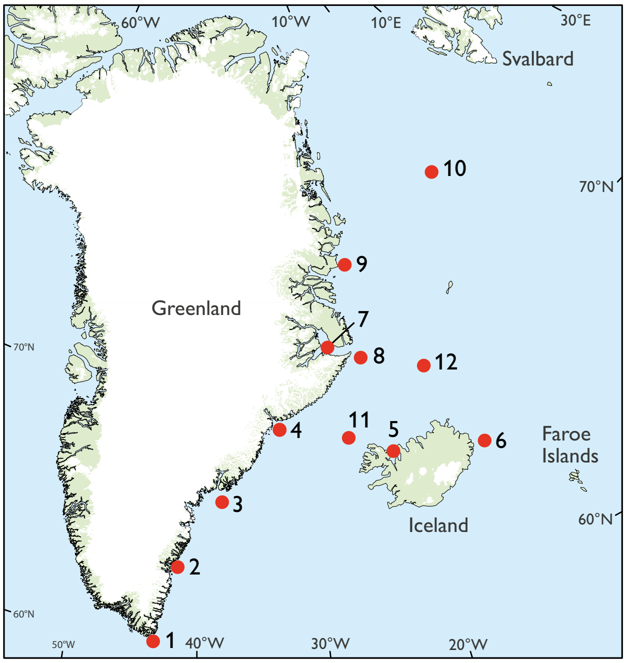

Fig. 3. Map of the location of the twelve points used for the probability matrix.

For further analyses of the sea-ice data, 12 points were selected (Fig. 3) to pinpoint areas of interest in order to investigate if there is a relationship between the points. A conditional probability matrix (Table 2) was created to analyse the relationship between the 12 selected points using the digitised datasets described above. We calculated the probability that if there is sea ice at a given point then there is sea ice at another point. For example, the value 0.177 in the last column indicates that if point 12 has sea ice then there is a 0.177 probability that point 11 also has sea ice. A strong probability is defined as a value of 0.850 to 1.000, a medium probability is defined as a value of 0.490 to 0.849 and a weak probability is less than 0.490.

Results

In this section, we discuss the observed relationship between the East Greenland sea ice and the sea ice off Iceland using nine probability maps and the conditional probability matrix (Table 2). Koch describes an A1 year as a year when the ice between Greenland and Iceland would have been narrow and Iceland free of ice throughout that year. During A1 years the probability maps show that sea ice would definitely have been present along the coast of Greenland, down to the southern tip with fluctuations out from the coast but the ice would not have reached Iceland. In A2 years, sea ice is approaching the north coast of Iceland, but Iceland itself would have been almost completely free of ice. It is further estimated that 80–100% of the time, sea ice would most likely have been at the northern part of the coast, and for only 60–79% of the time to be present at the southern part of Iceland. In A3 years the sea-ice belt would have been wider at times extending into the northern fjords of Iceland.

In B years, the sea ice would have formed a broad belt north of Iceland. Koch describes in his report that the ice edge reached near 67°N and 15°W, which corroborates the digitised data. In B1 years, the probability maps reflects a wider range of sea-ice extent along the coast of Greenland. For example, at Scoresby Sund (point 7), the maps show that the fjord is not always covered by ice during those years. In B2 years, the probability map shows that the probability of 80 to 100% covers a larger area along Greenland's east coast, and has an extent of sea ice that reached further along the

Table 2. A conditional probability matrix

Probability point has sea ice	Known point with sea ice: 1	2	3	4	5	6	7	8	9	10	11	12
1	1.000	0.916	0.896	0.942	0.789	0.625	0.889	0.898	0.880	0.969	0.828	0.169
2	0.924	1.000	0.948	0.942	0.842	0.500	0.937	0.933	0.930	0.984	0.841	0.171
3	0.896	0.940	1.000	0.919	0.789	0.625	0.913	0.918	0.907	0.977	0.832	0.168
4	0.976	0.976	0.960	1.000	0.842	0.500	0.980	0.988	0.981	0.977	0.845	0.165
5	0.060	0.064	0.060	0.062	1.000	0.750	0.063	0.063	0.062	0.094	0.082	0.316
6	0.020	0.016	0.020	0.015	0.316	1.000	0.016	0.016	0.016	0.031	0.026	0.375
7	0.900	0.940	0.924	0.950	0.842	0.500	1.000	0.961	0.946	0.961	0.823	0.163
8	0.920	0.948	0.940	0.969	0.842	0.500	0.972	1.000	0.965	0.984	0.845	0.169
9	0.912	0.956	0.940	0.973	0.842	0.500	0.968	0.976	1.000	0.984	0.828	0.167
10	0.498	0.502	0.502	0.481	0.632	0.500	0.488	0.494	0.488	1.000	0.509	0.305
11	0.771	0.777	0.775	0.754	1.000	0.750	0.758	0.769	0.744	0.922	1.000	0.177
12	0.977	1.000	0.977	1.000	0.140	0.070	0.953	1.000	1.000	0.907	0.953	1.000

The left hand column indicates the point with sea ice (in relation to Fig. 2), while the rows show the probability of sea ice present relative to that point

Icelandic northern coast. Unlike that observed in B1 years, for B2 years Scoresby Sund was often filled with sea ice. Finally, during C years, sea ice was present along the entire East Greenland coast and for 40–59% of the years the ice would extend down the eastern coast of Iceland.

Of the nine maps, the remaining three show sea-ice data off Iceland from 1877 to 1939. These maps provide more details on sea-ice extent during a more severe ice period in the 1880s (Kelly *et al.* 1987, based largely on Koch's index of Icelandic sea-ice occurrence). In B2 years, there was a 40 to 59% probability of sea ice reaching all along the northern coast of Iceland, but persisting mainly between Iceland and Greenland. The B3 years have a wider area between Greenland and Iceland and cover a further range along the northern Icelandic coast. Kelly *et al.* (1987) discuss three of the B3 years (1914, 1915 and 1938) as being years with extensive sea ice around Iceland. During C years, the sea ice extended to the south coast of Iceland. Seven of these years (1881, 1882, 1887, 1888, 1892, 1911 and 1918) were severe sea-ice years for Iceland (Kelly *et al.* 1987).

A statistical analysis was carried out to see if there is any correlation between sea ice being present at one point (Table 2) to other points on the map. The strongest probabilities are the points along eastern Greenland, points 1–4 and 7–9. This implies that if there is sea ice at one point along the coast then it is very likely that the rest of the eastern coast of Greenland would have been filled with ice. Point number 12 is located farther from the coast but has a perfect correlation with points 2, 4, 8 and 9 along the coast. The points farther from the coast 10–12 have a range of weak to strong probability with the other points. Point 12 also shows a relatively higher probability value of 0.316 and 0.375 with points 5 and 6 than the other points closer to Greenland, which all have weak values of less than 0.094.

Lauge Koch's index extends further back in time than the maps of the spatial extent. When using the probability maps, it is now possible to see how extensive the sea ice was likely to have been in the period from 1821 to 1893. The final application of the maps is to use them in combination with Table 1 to be able to estimate sea-ice extent back to 1821.

Conclusion

134 maps showing sea-ice extent from 1877 to 1939 are available as jpeg files and shapefiles. Detailed probability maps have been created from observed and estimated sea-ice conditions from observed data that date back to the early 1800s. These probability maps can be downloaded at *https://dx.doi.org/10.1594/PANGAEA.887452* where the maps are available as jpeg files. The datasets can be used in further studies to help understand the characteristics of sea ice during the 19th and 20th centuries. Previous studies have used Koch's sea-ice index to infer atmospheric circulation patterns (Kelly *et al.* 1987). Our new dataset can provide important input to studies of climatic variability in the (sub)Arctic including the link between ice and atmospheric circulation modes such as the Arctic and North Atlantic Oscillations (AO/NAO) and thus helps predicting how the climate may respond to future sea-ice loss (Screen *et al.* 2017).

References

Chapman, W.L. & Walsh, J.E. 1993: Recent variations of sea ice and air temperature in high latitudes. Bulletin of the American Meteorological Society **74**, 33–47.

Kelly, P.M., Goodess, C.M. & Cherry, B.S.G. 1987: The interpretation of the Icelandic sea ice record. Journal of Geophysical Research: Oceans **92**(C10), 10835–10843.

Koch, L. 1945: The East Greenland Ice. Meddelelser om Grønland **130**(3), 373 pp.

Screen, J.A. 2017: The missing northern European winter cooling response to Arctic sea ice loss. Nature communications **8**, 14603.

Thoroddsen, T. 1884: Den grönlandska drifisen vid Island. Ymer **1884**, 145–160.

Underhill, V., Fetterer, F. & Petersen, C. 2014: Arctic sea ice concentration and extent from Danish Meteorological Institute sea ice charts, 1901–1956, Version 1. Boulder: NSIDC (National Snow and Ice Data Center), *https://dx.doi.org/10.7265/N5MP517M*

Vaughan, D.G. *et al.* 2013: Observations: Cryosphere. In: Stocker, T.F. *et al.* (eds): Climate Change 2013: The Physical Science Basis. Contribution of working group I to the Fifth Assessment Report of the Intergovernmental Panel on Climate Change, 317–382. Cambridge: Cambridge University Press.

Walsh, J.E., Chapman, W.L. & Fetterer, F. 2015, updated 2016: Gridded monthly sea ice extent and concentration, 1850 onwards, Version 1.1, Boulder: National Snow and Ice Data Center. Digital media, *http://dx.doi.org/10.7265/N5833PZ5*

Walsh, J.E., Fetterer, F., Stewart, J.S. & Chapman, W.L. 2017: A database for depicting Arctic sea ice variations back to 1850. Geographical Review **107**, 89–107, *http://dx.doi.org/10.1111/j.1931-0846.2016.12195.x*

Authors' address

Geological Survey of Denmark and Greenland, Øster Voldgade 10, DK-1350 Copenhagen K, Denmark. E-mail: *dhalle23@gmail.com*.